1-2003

Practical analysis of polymers with depth varying compositions using Fourier transform infrared photoacoustic spectroscopy (plenary)

John F. McClelland
Iowa State University, mcclelland@ameslab.gov

Roger W. Jones
Iowa State University, jonesrw@ameslab.gov

Siquan Luo
Iowa State University

Practical analysis of polymers with depth varying compositions using Fourier transform infrared photoacoustic spectroscopy (plenary)

Abstract
Fourier transform infrared photoacoustic spectroscopy can be used as a nondestructive method to probe the molecular composition of materials as a function of depth into the sample. This is done by varying the thickness of the surface layer being analyzed, which can be as great as some tens of micrometers, depending on optical and thermal properties.Computational methods are described to process photoacoustic amplitude and phase spectra for both semiquantitative and quantitative depth analyses. These methods are demonstrated on layered and gradient samples.

Keywords
Biochemistry Biophysics and Molecular Biology, Mechanical Engineering, Fourier transforms, materials analysis, photoacoustic spectroscopy, spectrum analysis, computational methods

Comments
The following article appeared in *Review of Scientific Instruments* 74 (2003): 285 and may be found at doi:10.1063/1.1516244.

AIP | Review of Scientific Instruments

Practical analysis of polymers with depth varying compositions using Fourier transform infrared photoacoustic spectroscopy (plenary)

John F. McClelland, Roger W. Jones, and Siquan Luo

Citation: Review of Scientific Instruments **74**, 285 (2003); doi: 10.1063/1.1516244
View online: http://dx.doi.org/10.1063/1.1516244
View Table of Contents: http://scitation.aip.org/content/aip/journal/rsi/74/1?ver=pdfcov
Published by the AIP Publishing

Practical analysis of polymers with depth varying compositions using Fourier transform infrared photoacoustic spectroscopy (plenary)

John F. McClelland,[a] Roger W. Jones, and Siquan Luo
Ames Laboratory, Iowa State University, Ames, Iowa 50011-3020 and MTEC Photoacoustics, Inc., Ames, Iowa 50014

(Presented on 24 June 2002)

Fourier transform infrared photoacoustic spectroscopy can be used as a nondestructive method to probe the molecular composition of materials as a function of depth into the sample. This is done by varying the thickness of the surface layer being analyzed, which can be as great as some tens of micrometers, depending on optical and thermal properties. Computational methods are described to process photoacoustic amplitude and phase spectra for both semiquantitative and quantitative depth analyses. These methods are demonstrated on layered and gradient samples. © *2003 American Institute of Physics.* [DOI: 10.1063/1.1516244]

I. INTRODUCTION

Materials with depth-varying molecular composition play an important role in both manmade and natural products. For example, coating systems, multilayer polymer packaging films, and medical devices, as well as numerous biological materials, utilize various gradient or layered structures to achieve desired functions. Spectroscopic molecular analysis probes are needed to characterize such materials nondestructively with a surface-to-bulk probe-depth range of tens of micrometers and a depth resolution varying from fractions of a micrometer to several micrometers. The capability to analyze both planar and nonplanar samples is desirable.

Infrared spectroscopic measurements based on reflection and transmission do not offer a nondestructive way to vary probe depth over the depth range of interest. Confocal Raman microscopy allows detection of Raman emission from small volume elements below the sample surface. Its capabilities and limitations, however, are not the subject of this article, which focuses on the use of Fourier transform infrared (FTIR) photoacoustic spectroscopy (PAS) for studying layered and gradient samples.

FTIR PAS is ideally suited for depth analysis because of the role of thermal waves in photoacoustic signal generation. Their short and externally controllable decay distances within the sample determine the layer thickness below the sample surface from which the signal is detected. Various numerical techniques have been developed to take advantage of this, and some of these will be discussed here. The thickness range extends from submicrometer to tens of micrometers. Furthermore, the propagation time of thermal waves within the sample gives depth-specific information because signals generated by molecular absorption deep within the sample are delayed in time relative to those produced by absorption closer to the surface.

[a]Electronic mail: mcclelland@ameslab.gov

II. PHOTOACOUSTIC SIGNAL GENERATION CONSIDERATIONS IN DEPTH ANALYSIS

The PAS signal generation sequence starts with the infrared beam of the FTIR spectrometer being incident on the sample and the nonreflected beam component penetrating into the sample a distance approximately equal to $1/\alpha$, where α is the sample optical absorption coefficient.[1,2] Absorption and thermalization of the light, which is intensity modulated by the interferometer, result in instantaneous temperature oscillations within the sample. The instantaneous oscillation amplitudes, excited at a particular radiation wave number, decay exponentially with depth into the sample according to the value of α at that wave number. Each layer of the sample that absorbs light and experiences temperature oscillations generates thermal waves with a decay coefficient given by $a_s=(\pi f/D)^{1/2}$, where f is the experimentally controllable light-intensity modulation frequency, and D is the sample thermal diffusivity.[1] These absorption-generated thermal waves propagate back in part to the incident beam surface and also cause the gas atmosphere in contact with the surface to oscillate in temperature. This results in pressure oscillations in the small-volume sample chamber of the photoacoustic detector, which are detected by a sensitive microphone as the photoacoustic signal. The amplitude of the pressure oscillations increases with α, thus allowing the relative sample absorbance to be measured.

In the range where α is less than or approximately equal to a_s, the probe depth is approximately equal to the thermal diffusion length, $L=1/a_s=(D/\pi f)^{1/2}$, because thermal waves generated deeper than L make a minor contribution to the temperature oscillations in the gas. L can be adjusted by changing the beam intensity modulation frequency, f, over a wide range. If α increases to values larger than a_s, the probe depth becomes limited by the decay of light rather than by the decay of thermal waves within the sample.

Table I gives thermal-wave propagation parameters[2] for a range of frequencies including: L; VT [the distance that a thermal wave travels in one oscillation period, $T=1/f$, with a velocity, $V=(4\pi Df)^{1/2}$]; and t/θ_t, which represents the

TABLE I. Thermal wave propagation parameters for different modulation frequencies (for $D=10^{-3}$ cm^2/s).

f (Hz)	L (μm)	VT (μm)	t/θ_t (μm/degree)
1	178	1120	3.1
10	56.4	354	0.98
50	25.2	159	0.44
100	17.8	112	0.31
400	8.92	56.0	0.16
1000	5.64	35.4	0.10
10000	1.78	11.2	0.031

number of micrometers that a thermal wave travels in the sample per degree of phase delay. For instance, at 100 Hz it can be seen in Table I that a thermal wave experiences a 10° phase delay crossing a 3.1 μm thick layer.

The decay of thermal waves within the sample and their role in phase delay allow probing of layers of variable thickness below the sample surface. Variations in layered and gradient compositions are revealed as the probe depth is increased by reducing the modulation frequency. A number of factors must be considered, however, in interpreting photoacoustic spectra measured at different frequencies and phase delays. In rapid-scan FTIR measurements, the interferometer optical-path-difference velocity, v, determines L according to the formula $L=(D/\pi\nu v)^{1/2}$, where ν is the wave number of a particular point in the spectrum. Consequently, in rapid-scan measurements, L varies across the spectrum. Alternatively, if step-scan FTIR measurements are made, the modulation frequency is determined by a phase modulation, which occurs when a small-amplitude oscillation occurs in the position of one of the interferometer mirrors. This mode of operation produces a constant value of L across the spectrum and also offers easy access to the phase of the PAS signal, in addition to its amplitude.

The variable probe depth nature of PAS results in two factors that must be accounted for. The first is that spectra have increased saturation (truncation of strong bands) as L values are increased, just as transmission spectra do when the sample path length is increased. The spectral changes associated with increasing saturation can be difficult to distinguish from spectral changes caused by compositional changes observed as L increases. When sample conditions allow it, the simplest way to deal with saturation effects is to scale all of the depth-varying spectra so that the intensities are equal for a weak band associated with a major component that is known to have little depth variation. This scaling allows spectral changes from depth varying components to be observed semiquantitatively when spectral overlap is minimal and the absorbance bands of interest are weak. In many practical applications, such is not the case, or a more quantitative analysis is required. A general quantitative method to compensate for increasing saturation is described in the next section.

The second factor to be accounted for is that spectra measured at a given L value (or range of L values in a rapid-scan measurement) are representative of an average concentration (weighted by the exponential decay coefficients α and a_s) within the layer. In many instances, however, one needs to know concentration as a function of depth. Calculating concentration profiles from a group of PAS spectra taken at different L values is complicated by the general problem commonly encountered in inverse-theory problems in which solutions tend to be unstable and may lead to large prediction errors. In Sec. III an approach is described in which a functional form, based on supplemental information, is used to stabilize the profile calculation.

The phase component of the photoacoustic signal also has important compositional information related to depth. The phase delay for a very strong absorbance peak approaches a phase shift of 90°, whereas a very weak absorbance has an ~135° phase shift relative to the excitation waveform for a homogeneous sample.[1] Nonhomogeneous samples can have both smaller or larger phase shifts than is the case for homogeneous samples, depending on the thermal, optical, and dimensional properties of the sample and the modulation frequency. In the case of layered samples, all of the phase delays associated with the absorbance bands of a particular layer are clustered within the same range of phase-shift angles with the first layer's cluster having the least delay, the next deeper layer cluster the next-to-the-least delay, etc.[3] This sequencing of layer clusters allows the layer order of multilayer films to be determined, as will be shown in a later section.

Since the PAS signal has amplitude and phase components, it is a vector quantity, which in the case of a two-layer structure allows the separation of the superimposed signals from the two layers by looking at orthogonal components of the signal. Another useful procedure is to use the amplitude and phase to calculate a linearized photoacoustic spectrum that has less saturation than a conventional magnitude spectrum. This procedure is described in Sec. III and an application example is presented in Sec. IV on the use of linearization.

III. SIGNAL PROCESSING FOR DEPTH ANALYSIS

A. Saturation equalization (Ref. 4)

Most data-processing methods aimed at depth analysis make use of phase information, but the earliest method was the direct comparison of spectra taken at different scanning speeds or modulation frequencies, which, as previously discussed, result in different thermal diffusion lengths, L, and so different effective probe depths. An example of this is presented in Sec. IV A. The difficulty with this is the increase in spectral saturation that accompanies lowering the scan speed or frequency. Fortunately, it is possible to remove most of the saturation differences between low and high scanning-speed spectra so that they may be more readily compared. A low-speed (or frequency) spectrum can be converted into a spectrum with the amount of saturation of a high-speed (or frequency) spectrum using the theory for photoacoustic signal generation in homogeneous samples.[1,5] This removes the saturation differences between spectra at different speeds or frequencies while retaining any differences related to sample structure. The idea is to use a spectrum peak, G, that is known to arise from a homogeneous component in the sample as a guide for reducing the amount of saturation in

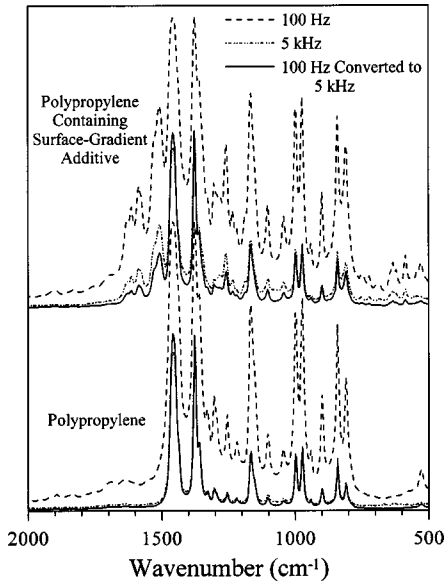

FIG. 1. Spectra of polypropylene with and without a near-surface additive. In each case, the low-speed (100 Hz) spectrum is transformed so as to have the same amount of saturation as the high-speed (5 kHz) spectrum. In the homogeneous sample, the converted spectrum matches the high-speed spectrum. In the other, the gradient of the additive makes the additive peaks smaller in the converted spectrum than in the high-speed spectrum.

the low-speed (or frequency) spectrum.[4] For a homogeneous component and normalized spectra, the ratio, $\mathbf{R}_n$, of the signal at a given wave number in a high-speed spectrum, $\mathbf{Q}_h$, to that in a low-speed spectrum, $\mathbf{Q}_l$, depends only on the ratio of the two speeds (high/low), N, and how much saturation is present. The guide peak, G, is used to determine the amount of saturation. The maximum photoacoustic signal, $\mathbf{Q}_{\max}$, occurs at full saturation, so a spectrum can be rescaled so that a value of 1 equals total saturation by dividing each point in the spectrum by $\mathbf{Q}_{\max}$. This scaled signal, $\mathbf{Q}_{sc}$, can then be related to $\mathbf{R}_n$:[4]

$$\mathbf{Q}_{sc}=\frac{\mathbf{Q}}{\mathbf{Q}_{\max}}=\frac{N^{1/2}\mathbf{R}_n-1}{\mathbf{R}_n(N^{1/2}-1)}, \tag{1}$$

$$\mathbf{R}_n=\frac{1}{N^{1/2}+\mathbf{Q}_{sc}(1\text{-}N^{1/2})}. \tag{2}$$

Equations (1) and (2) involve the vectors $\mathbf{Q}_{sc}$ and $\mathbf{R}_n$ (as well as $\mathbf{Q}$ and $\mathbf{Q}_{\max}$), which include phase, but they can be converted to analogous, but substantially more complicated, equations for the signal magnitudes, Q_{sc} and R_n. These equations are given in Ref. 4.

G guides the conversion of a high-saturation, low-speed spectrum into a low-saturation, high-speed-equivalent spectrum that retains the probe depth (thermal diffusion length) of the low speed. First, high- and low-speed spectra are acquired from a sample. The ratio R_n is determined for G from its magnitudes in the observed high-speed and low-speed spectra, then the value of Q_{sc} for G is calculated from the magnitude analog of Eq. (1). This establishes the Q_{sc} values for the whole spectrum because it is just a linear scaling. Substituting the Q_{sc} values into the analog of Eq. (2) then gives R_n values for the whole spectrum. Multiplying the data points in the low-speed spectrum by their R_n values results in the high-speed-equivalent spectrum.

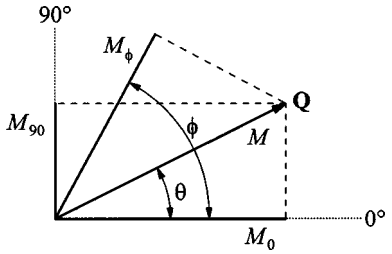

FIG. 2. Relationships of the photoacoustic signal vector, $\mathbf{Q}$, with its magnitude, M, and phase, θ, to the orthogonal component magnitudes, M_0 and M_{90}, and the magnitude, M_ϕ, observed at a detection angle of ϕ.

Figure 1 shows the conversion process applied to two different samples. Spectra of a homogeneous polypropylene sample are at the bottom, and above them are spectra of polypropylene containing an additive that has been diffused in from the sample surface, so it is concentrated near the surface. In each group, the dashed and dash-double-dot spectra were taken at scanning speeds of 100 Hz and 5 kHz (laser-fringe speeds, equivalent to 0.0063 and 0.032 cm/s OPD velocities). In both sets, the solid-line spectrum is the 100 Hz spectrum after conversion to 5 kHz equivalence. For the pure polypropylene, the true 5 kHz spectrum and the converted spectrum are close matches, as they should be if the saturation levels have been equalized. For the sample containing the additive, the heights of the polypropylene bands match in the 5 kHz and converted spectra but the additional bands from the additive do not; they are distinctly stronger in the true 5 kHz spectrum, indicating that the concentration of the additive drops off with sample depth. A quantitative example of applying this saturation-equalization method is described in Sec. IV B.

B. Phase calculation

With the advent of phase-modulation (commonly called step-scan) FTIR spectrometers, using phase for photoacoustic depth profiling became more common because phase modulation provides ready access to both the magnitude and phase of the photoacoustic signal vector. Figure 2 shows the relationship among the various vectors and measurements involved. The photoacoustic signal vector, $\mathbf{Q}$, at a given wave number has a magnitude, M, and an observed phase, θ. This observed phase is not the same as the true photoacoustic phase because it also contains contributions from the spectrometer and depends on where the spectrometer defines 0°. Many spectrometers allow either the sample itself or some other reference material to be used as the phase reference. Zero degrees will then be set equal to the phase of that reference. If the sample itself is used, then $\theta=0°$, and no useful phase information is retained. More usefully, the reference can be a thermally thick sample that absorbs all infrared radiation right at the surface. The phase for such a reference will be as fast as possible for thermally thick, homogenous material, so all thermally thick, homogenous samples will

lag behind it by between 0° and 45°.[1,5] Layered samples can have phases outside this range. We have found glassy carbon to be a good choice for such a reference.[6]

When phase-modulation spectra are acquired, the spectrometer typically produces two orthogonal component spectra, which have magnitudes M_0 and M_{90} at a given wave number and are the projections of **Q** onto the 0° and 90° axes, as shown in Fig. 2. The magnitude and phase of the photoacoustic signal are then typically calculated this way:

$$M=(M_0^2+M_{90}^2)^{1/2}, \tag{3}$$

$$\theta=\tan^{-1}\left(\frac{M_{90}}{M_0}\right). \tag{4}$$

It should be kept in mind that the usual Fourier transform process typically causes M_0 and M_{90} to be positive valued at all wave numbers, and this forces θ to be between 0° and 90° when Eq. (4) is used. The actual value of θ may be outside this range for layered and other structured samples. Using interferograms to determine phase can mitigate this problem somewhat because it allows θ to have a 180° range.[2,7]

In the analysis of layered samples, it is often advantageous to determine the sample spectrum at a specific detection phase angle, in the manner of a lock-in amplifier. For example, proper choice of the detection angle can isolate the spectrum of one layer in a two-layer sample. The spectrum at a specific angle, ϕ, is a projection of **Q** onto the ϕ axis, as shown in Fig. 2, and is related in the following manner to the other quantities discussed:

$$M_\phi=M\cos(\phi-\theta)=M_0\cos\phi+M_{90}\sin\phi. \tag{5}$$

C. Linearization

The strongest peaks in most FTIR photoacoustic spectra show some saturation effects (i.e., a sublinear dependence of signal magnitude on the absorption coefficient). The onset of saturation for homogeneous samples is moderately low, occurring roughly when the absorption coefficient, α, equals $1/(10L)$, where L is the thermal diffusion length. Increasing the scanning speed or modulation frequency will lower L and reduce saturation, but often this cannot be done. Saturation increases only gradually with increasing α, however, so full saturation does not occur until about $\alpha=20/L$, and useful spectra can be acquired out to near this limit. Fortunately, the range over which partial saturation occurs is also the range where the phase of the photoacoustic signal is most sensitive to the absorption coefficient,[8] so phase can be used to correct the magnitude spectrum for saturation; that is, to *linearize* it. The linearized spectrum, q_{lin}, can be calculated from the real and imaginary component spectra of the sample and a phase reference:[9]

$$q_{\text{lin}}=\frac{q_s^2}{R_sI_r-I_sR_r}, \tag{6}$$

where q_s is the observed (partly saturated) sample spectrum, R_s and I_s are the real and imaginary components of the sample spectrum, and R_r and I_r are the real and imaginary components of the phase-reference spectrum. The phase reference, like that for phase-modulation spectra, must absorb the spectrometer beam right at its surface, so that it produces the earliest possible photoacoustic phase for a thick, homogeneous sample. Again, glassy carbon has proven to be a good choice.[6]

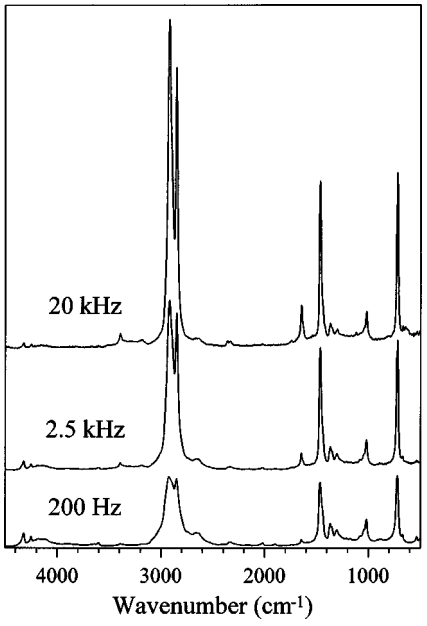

FIG. 3. Spectra taken at the three marked scanning speeds of polyethylene pellets containing two additives, one uniformly dispersed and the other concentrated at the surface. Increasing speed both reduces saturation on the larger polyethylene peaks, causing them to grow, and reduces the photoacoustic probe depth, causing the surface-additive peak at 1650 cm^{-1} to grow as well. The uniform-additive peak at 1020 cm^{-1}, however, remains unchanged. The spectra have been scaled so that the small 1370 cm^{-1} peak is of constant size.

What relevance does spectrum linearization have to depth-variation analysis? The greater the amount of saturation in a peak, the earlier its phase, so in the linearization process the earlier the phase is for a peak, the greater its observed magnitude is increased to restore linearity. For a nonhomogeneous sample, the spectrum bands arising from any species concentrated at or near the sample surface will have particularly early phases, so when the spectrum is linearized, these surface-species bands enlarge disproportionately and are easily picked out. An example of this is discussed below in Sec. IV C.

IV. APPLICATION EXAMPLES

A. Polymer additives

Additives are often mixed into polymers to provide improved surface and bulk properties for specific applications. Surface additives are engineered to migrate to the surface and provide properties such as lubrication for mold release or static-charge reduction, whereas bulk additives often stabilize polymers to withstand ultraviolet radiation or thermal stress. Figure 3 shows variable probe-depth spectra of polyethylene polymer pellets containing both surface segregating and bulk additives. These spectra were scaled so that the polyethylene band at 1370 cm^{-1} is of equal height in all spectra to reduce saturation effects for the weaker bands.

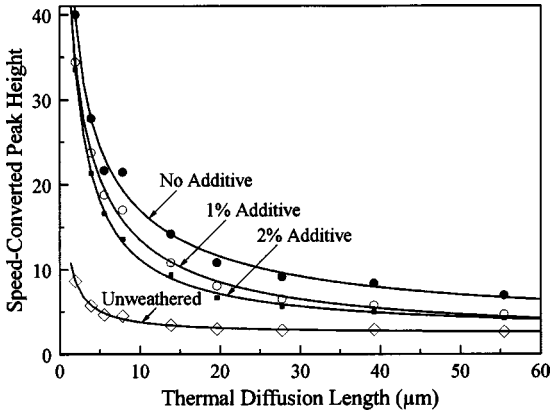

FIG. 4. Markers are observed peak heights for a hydroxyl band at $3271\,\mathrm{cm}^{-1}$ in spectra of weathered PET samples containing various amounts of an ultraviolet-protection additive. The spectra were taken at various scanning speeds and then saturation equalized. The equalization process reveals the intrinsic drop off with thermal diffusion length of the hydroxyl peaks, which would normally be masked by a saturation-induced increase in overall signal strength. The lines are least-squares fits to the data, assuming the hydroxyl concentration profiles are double exponentials.

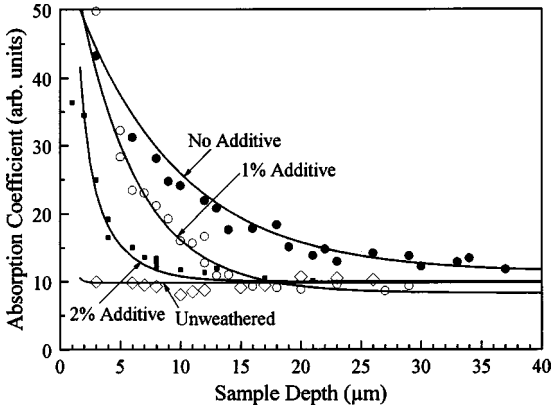

FIG. 5. Lines are depth profiles for hydroxyl in weathered PET derived from the fits in Fig. 4. The markers are confirming measurements of peak heights at a single, high scanning speed made as the samples were lapped off to reveal successive depths within the original, intact material. All four depth profiles have been scaled by the same amount to match the ordinate scale of the lapping measurements.

This scaling obviously is ineffective for the strong polyethylene band at $2900\,\mathrm{cm}^{-1}$, as well as the polyethylene bands at 1440 and $720\,\mathrm{cm}^{-1}$, all of which increase in height with decreasing L (increasing f) as the level of saturation decreases, despite the fact that their concentration is essentially constant with depth. On the other hand, the scaling allows the behavior of weak bands as a function of depth to be readily observed. The surface additive band at $1650\,\mathrm{cm}^{-1}$ is observed to grow with decreasing L, indicating higher concentration at the surface, while the bulk additive band at $1020\,\mathrm{cm}^{-1}$ remains constant, indicating a uniform concentration to a depth of $\sim 40\ \mu$m.

B. Polymer weathering

The scaling just described, while useful in some cases, is not sufficient as a general method to compensate for saturation differences as a function of L. A general method to compensate for saturation differences in spectra, as described in the last section, was applied to weathering studies of PET polymers containing different concentrations of an ultraviolet stabilizer. Figure 4 shows saturation-compensated peak-height points of the $3271\,\mathrm{cm}^{-1}$ hydroxyl absorbance band plotted as a function of L for weathered samples having 0%, 1%, and 2% ultraviolet stabilizer concentrations and for an unweathered sample. The curves in Fig. 4 are least-squares fits to the data points of the photoacoustic signal equation:

$$S = C\left(c_0 + \sum_{i=1}^{n} \frac{c_i}{1-d_i}\right), \tag{7}$$

with $n=2$, where C, c_0, c_i, and d_i are fitting constants. Equation (7) is the form expected for gradients consisting of a sum of exponentials:[4]

$$\alpha(x) = c_0 + \sum_{i=1}^{n} c_i e^{d_i x}, \tag{8}$$

where x is depth. Once the fitting constants are obtained from the least-squares fits to the data in Fig. 4, absorption coefficient versus sample-depth curves can be calculated from Eq. (8), as shown in Fig. 5. The points shown in Fig. 5 were obtained from lapping measurements and are in close agreement with the calculated curves, confirming the photoacoustic analysis.

C. Linearization for high surface specificity

Linearized photoacoustic spectra accentuate the photoacoustic signal components generated closest to the surface and result in spectra that are similar to what would be measured if the modulation frequency were increased by approximately a factor of 10. Figure 6 illustrates this for the same polyethylene sample containing additives which was discussed earlier. Comparison of Figs. 3 and 6 shows that the

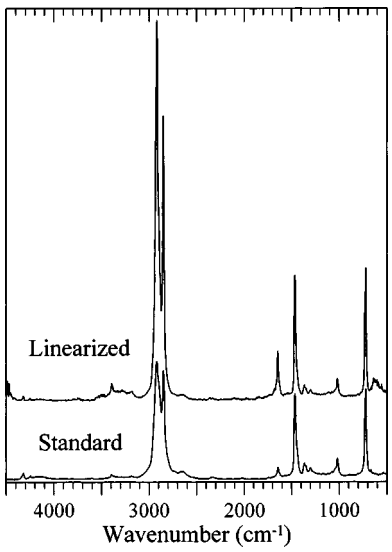

FIG. 6. Effect of linearization on the spectrum of the same polyethylene-with-additives sample used for Fig. 3. Linearization acts like increasing the scanning speed by reducing saturation in large peaks and emphasizing bands of near-surface species, such as the $1650\,\mathrm{cm}^{-1}$ band of the surface-concentrating additive.

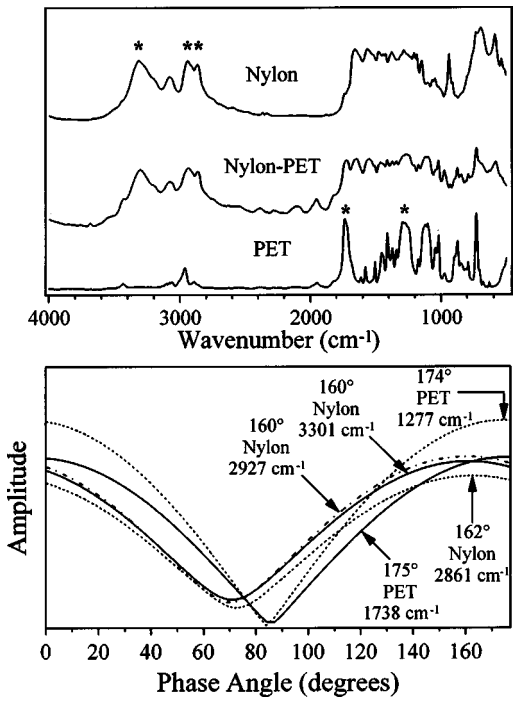

FIG. 7. Upper panel: spectrum of a single nylon-coated PET fiber compared to reference spectra of nylon and PET. Lower panel: magnitudes of the bands marked in the upper panel shown as a function of detection angle. The PET bands all clearly peak at later (higher) angles because the energy deposited in the PET must transit through the nylon coating before generating a photoacoustic signal.

surface-segregating additive and the bulk-additive absorbance bands behave the same as the sampling-depth changes in the two figures. In the case of Fig. 6, the standard magnitude spectrum and the linearized spectrum were both calculated from a single, simultaneous acquisition of the amplitude and phase spectra.

D. Multilayer analysis using phase

Phase analysis is applicable to both planar and nonplanar samples, including microsamples such as single fibers, which is illustrated in Fig. 7. The top panel of Fig. 7 shows the spectrum of a single nylon-coated PET fiber and reference spectra for nylon (above) and PET (below). The magnitudes of a series of nylon and PET absorbance bands are plotted as a function of detection angle in the bottom panel. These bands are all of approximately the same magnitude and would be expected to have their minima close together for a homogeneous sample. However, as discussed in Sec. II phase-angle minima for each layer of a layered sample are expected to cluster together, with the first-layer cluster having the smallest phase angles and deeper layers having progressively larger angles. This prediction is well illustrated in this example of a two component system.

V. CONCLUSIONS

This article has reviewed the use of FTIR photoacoustic spectroscopy as a means to nondestructively analyze the molecular composition of samples as a function of depth. The technique is shown to be applicable to both planar and nonplanar samples in macro- and microsizes. The ability of the technique to probe from the sample surface to experimentally controlled depths is due to the decay and finite-velocity properties of thermal waves, which are generated when the sample absorbs infrared radiation from the spectrometer.

A computational method was discussed that compensates for increases in spectral saturation (strong absorbance band truncation), which occur with increasing probe depth, so that spectral changes due to compositional changes with depth could be observed. A second computational method that provides higher surface specificity was described, which utilizes photoacoustic signal amplitude and phase data to linearize spectra and achieve the equivalent of a factor of 10 higher modulation frequency. A third method was outlined for plotting photoacoustic spectra as a function of phase detection angle, which allows phase shifts due, for instance, to thermal wave propagation across layers to be observed for analytical purposes.

Application examples were presented using: spectra measured at different frequencies and linearization to observe the depth distribution of additives in polyethylene; saturation compensation to determine the depth distribution of weathering-induced hydroxyl species in PET; and phase analysis to differentiate between the coating and fiber-core polymers of a single microfiber.

ACKNOWLEDGMENTS

The authors wish to thank Digilab for technical support and for loan of a FTIR spectrometer used for some of the work reported here. A portion of the work reported here was performed under CRADA No. AL-C-2000-01, jointly funded by the Office of Science of the U. S. Department of Energy, Ford Motor Company, Minnesota Mining and Manufacturing Company, Sherwin-Williams Company, and MTEC Photoacoustics, Inc. This work was funded in part by the Iowa State University of Science and Technology under Contract No. W-7405-ENG-82 with the U.S. Department of Energy. This work was funded in part by the Iowa State University of Science and Technology under Contract No. W-7405-ENG-82 with the U.S. Department of Energy. The United States Government retains and the publisher, by accepting the article for publication, acknowledges that the U.S. Government retains a nonexclusive, paidup, irrevocable, worldwide license to publish or reproduce the published form of this manuscript, or allow others to do so, for U.S. Government purposes.

[1] A. Rosencwaig and A. Gersho, J. Appl. Phys. **47**, 64 (1976).
[2] J. F. McClelland, R. W. Jones, and S. J. Bajic, *Handbook of Vibrational Spectroscopy*, edited by J. M. Chalmers and P. R. Griffiths (Wiley, Chichester, UK, 2002), Vol. 2, p. 1231.
[3] E. Y. Jiang, R. A. Palmer, and J. L. Chao, J. Appl. Phys. **78**, 460 (1995).
[4] R. W. Jones and J. F. McClelland, Appl. Spectrosc. **56**, 409 (2002).
[5] F. A. McDonald and G. C. Wetsel, Jr., J. Appl. Phys. **49**, 2313 (1978).
[6] R. W. Jones and J. F. McClelland, Appl. Spectrosc. **55**, 1360 (2001).
[7] R. W. Jones and J. F. McClelland, Appl. Spectrosc. **50**, 1258 (1996).
[8] Y. C. Teng and B. S. H. Royce, J. Opt. Soc. Am. **70**, 557 (1980).
[9] R. O. Carter III, Appl. Spectrosc. **46**, 219 (1992).